Atom vortex beams

V. E. Lembessis,[1] D. Ellinas,[2] M. Babiker,[3,*] and O. Al-Dossary[1,4]

[1]*Department of Physics and Astronomy, College of Science, King Saud University, Riyadh 11451, Saudi Arabia*

[2]*School of Electronic & Computer Engineering, Technical University of Crete, Crete, GR 73 100, Greece*

[3]*Department of Physics, University of York, Heslington, York YO10 5DD, United Kingdom*

[4]*National Centre for Applied Physics, KACST, P.O. Box 6086, Riyadh 11442, Saudi Arabia*

(Received 23 December 2013; published 15 May 2014)

The concept that all de Broglie particles can form vortex beams is analyzed for neutral atoms. It is shown how atoms diffracted from a suitably constructed optical mask configuration employing light of l units of orbital angular momentum and at far-off resonance with an atomic transition can lead to the generation of a discrete set of atom vortex beams each endowed with the property of quantized orbital angular momentum about the beam axis in units of $\hbar l$. Selection criteria of atom vortex beams are derived and the functioning of the mask configuration for angular dispersion of beams in terms of de Broglie wavelength is analyzed. Prospects of applications in the areas of atom interferometry and dispersion, and quantum information processing via atom vortices are pointed out.

DOI: 10.1103/PhysRevA.89.053616 PACS number(s): 03.75.Be, 42.50.Tx

The study of optical vortex beams and their applications have received much attention in recent years [1–6], and there are various types of optical vortex beams, in each of which the fields are characterized by the phase factor $e^{il\phi}$, where l is the vortex integer winding number and ϕ is the azimuthal angle about the beam axis. The influence of optical vortex beams on bulk matter has led to a number of applications, including the optical spanner effect, which acts to rotate small material particles immersed in the optical vortex in analogy to the optical tweezer effect, which influences their translational motion [2].

In addition to their action on small matter particles, optical vortex beams also have mechanical effects on atoms, ions, and molecules. Such effects have been subjected to both theoretical and experimental investigations. Optical vortices acting on the atomic center of mass generate a light-induced torque [7], which results in the rotational motion, while atoms subject to multiple optical vortex beams are known to reveal interesting patterns, including the creation of micron-size neutral or charged current loops [8–11], and optical Ferris wheels [12]. More recently, cold atoms have been trapped in a doughnut LG beam creating a persistent atomic current [13].

Emphasis has recently shifted to the creation in the laboratory of electron vortex beams [14–20], in analogy with optical vortex beams. Electron vortex beams are also endowed with the property of orbital angular momentum and they are characterized by a wave function bearing the phase factor $e^{il\phi}$, as appears in the case of the optical vortex fields. However, there are marked differences of electron vortices when compared to optical vortices in that electron vortices are characterized by the electron mass, electronic charge, and electron spin, all of which introduce new effects that are absent in the optical vortex case. Studies of electron vortices and their interaction with matter are now progressing in both the theoretical and experimental fronts.

The concept of a vortex beam should apply to any de Broglie particle and this includes atoms, ions, and molecules provided that each can be produced in the form of an initial well-defined ordinary beam, but it is unclear how one can generate the particle vortex in the case of a neutral atom beam. In both optical and electron vortices the production relies on the generation of a material computer-generated mask and diffraction is the physical process through which the vortex beams are realized.

To create atom vortex beams we need a suitable mask and here we propose and analyze the use of an optical mask suitably constructed from laser light as a diffracting agent. The situation is illustrated in Fig. 1, for the case of a forklike mask, which should be straightforward to set up in the laboratory, created by the superposition of a Laguerre-Gaussian laser beam with a reference plane wave, both plane polarized along the y axis. The incident LG optical beam is taken to propagate along the z axis (out of the plane), while the reference plane-wave laser beam is tilted at an angle α in the x-z plane, as shown in Fig. 1.

The total electric field is given by $\mathbf{E}(x,y,z) = \widehat{\mathbf{y}}\mathcal{E}(x,y,z)$, where $\mathcal{E}$ is the field distribution given by the sum

$$\mathcal{E}(x,y,z) = \mathcal{E}_P e^{-ik_x x} e^{-ik_z z} + \mathcal{E}_{\mathrm{LG}} f(r) e^{-il\phi} e^{-ik_z z}, \qquad (1)$$

where $\mathcal{E}_P$ is the plane-wave amplitude and $\mathcal{E}_{\mathrm{LG}}$ is the amplitude of the LG beam given by $\mathcal{E}_{\mathrm{LG}} = E_{00}(2/\pi|l|)^{1/2}$ with l the winding number of the LG mode, $k_x = k\cos\alpha$, $k_z = k\sin\alpha$, where k the wave number of the light and $r = \sqrt{x^2+y^2}$. The function $f(r,z)$ for a LG beam with $p = 0$ (so-called doughnut beam in the case of a large Rayleigh range), is given by

$$f_{|l|}(r) = \left(\frac{r\sqrt{2}}{w_0}\right)^{|l|} e^{-r^2/w_0^2}, \qquad (2)$$

where w_0 is the waist at focus where $z = 0$. The forklike mask corresponding to the electric field (1) is shown in Fig. 2 for the case of a doughnut LG beam with $l = 1$.

A two-level atom interacting with the above field has a z-independent Rabi frequency given by

$$\Omega^2(r,\phi) = \Omega_P^2 + \Omega_{\mathrm{LG}}^2 f^2(r) + 2\Omega_P\Omega_{\mathrm{LG}} f(r)\cos(k_x x - l\phi), \qquad (3)$$

*Corresponding author: m.babiker@york.ac.uk

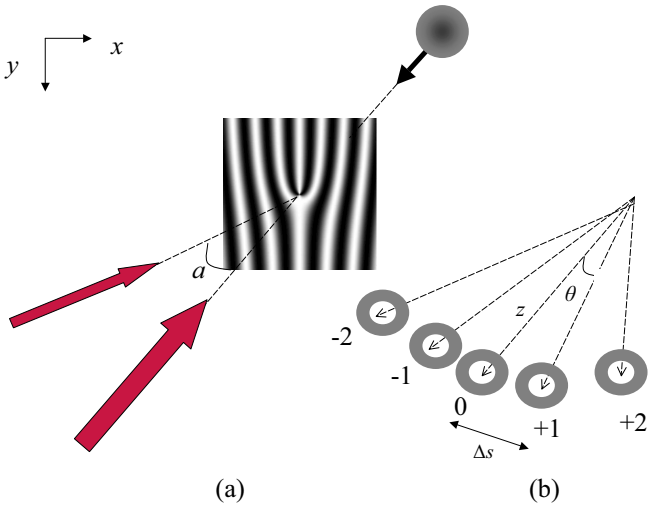

FIG. 1. (Color online) (a) Schematic representation of the diffraction of the atoms through the light mask made up of a Laguerre-Gaussian doughnut beam of winding number l interfering with a tilted plane wave $l = 2$; (b) after the diffraction process the different atom vortices are shown separated in space and are labeled $n = 0, \pm 1 \pm 2, \ldots$ with the nth vortex carrying orbital angular momentum $nl\hbar$.

where Ω_P and $\Omega_{\rm LG}$ are the Rabi frequencies associated with the plane wave and the Laguerre-Gaussian beam, respectively. As a result of acquiring this Rabi frequency once subject to the mask fields, the atom experiences an optical dipole potential. This dipole potential in the case of far detuning $\Delta = \omega - \omega_0$, with ω and ω_0 the frequency of the light and that of the atomic transition, respectively, such that $\Omega/\Delta \ll 1$, is given by

$$U(r,\phi) = -\frac{2\hbar\Omega^2(r,\phi)}{\Delta}. \tag{4}$$

Since the detuning is assumed relatively large, the above potential effectively acts on the atom in its ground state and

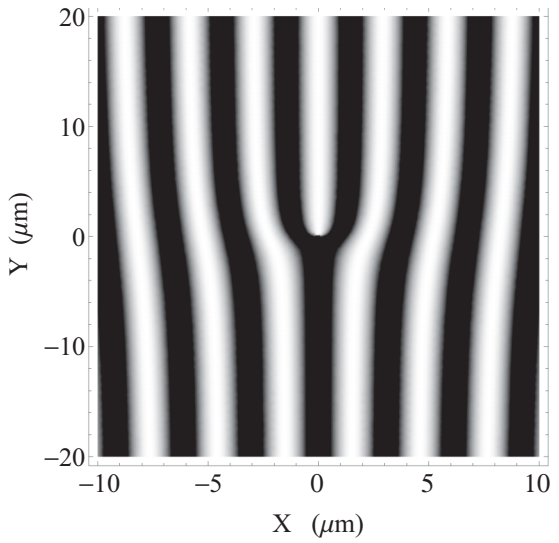

FIG. 2. The forklike light mask displaying the intensity of the field given by Eq. (1), for a winding number $l = 1$. Lighter gray areas correspond to higher intensity.

results in its diffraction over a short interaction time τ. We assume that the atom enters the potential at the time $t = -\tau$ and its state function at that instant is $\Psi(r,\phi,-\tau)$. After the diffraction the atomic state function is at time $t = 0$ and is given by

$$\Psi(r,\phi,0) = \Psi(r,\phi,-\tau)e^{iU\tau}. \tag{5}$$

On substituting for U from Eq. (4) we have

$$\Psi(r,\phi,0) = \Psi(r,\phi,-\tau)\exp\left(-\frac{i2\tau}{\Delta}\Omega^2(r,\phi)\right). \tag{6}$$

The physical interpretation of the above expression is that the diffraction process through the optical potential over the short period of time τ is in the form of a phase imprint on the initial wave function. This is the basic principle of vortex sorting in Bose-Einstein condensates. Substituting for Ω from Eq. (3) we have

$$\Psi(r,\phi,0) = \Psi(r,\phi,-\tau)e^{-iA\tau}e^{-iB\tau}e^{-iC\tau\cos(k_x x - l\phi)}, \tag{7}$$

where $A(r), B(r)$, and $C(r)$ are functions of r only

$$A = \frac{2}{\Delta}\Omega_P^2; \quad B = \frac{2}{\Delta}\Omega_{\rm LG}^2 f_{|l|}^2; \quad C = \frac{\Omega_p\Omega_{\rm LG}}{\Delta}f_{|l|}. \tag{8}$$

The last exponential factor in Eq. (7) involving dependence on k_x and ϕ can be expressed as a sum over Bessel functions using the Jacobi-Anger identity, $e^{iz\cos\theta} = \sum_{-\infty}^{\infty} i^n J_n(z)e^{in\theta}$, and yields

$$\Psi(r,\phi,0) = \Psi(r,\phi,-\tau)e^{-iA\tau}e^{-iB\tau} \times \sum_{-\infty}^{\infty} i^n J_n(C\tau)e^{-ink_x x}e^{inl\phi}. \tag{9}$$

The initial-state function of the atoms prior to entering the interaction region (i.e., at time $t = -\tau$) is best discussed with reference to a practical scenario involving a cold atomic wave packet. This wave packet is assumed to have a transverse Gaussian profile with a typical cross section of dimensions of the order of tens of microns [21]. Thus we can write $\Psi(r,\phi,z,-\tau) = \mathcal{N}D(r)e^{ik_z^{dB}z}$, where $D(r) = \exp(-\frac{4\ln 2}{\sigma^2}r^2)$, where σ is the transverse size of the atomic wave packet, as schematically represented in Fig. 1, k_z^{dB} is the atomic de Broglie wave vector along the z direction, and $\mathcal{N}$ is the normalization constant. The wave function now reads

$$\Psi(r,\phi,0) = \mathcal{N}e^{-iA(r)\tau}e^{-iB(r)\tau}D(r) \times \sum_{n=-\infty}^{\infty} i^n J_n(C\tau)e^{-i(nk_x x - k_z^{dB}z)}e^{inl\phi}. \tag{10}$$

Equation (10) shows that the diffracted wave function is a superposition of atom states indexed by integers $n = 0, \pm 1, \pm 2, \ldots$, each endowed with angular momentum $n\hbar l$ propagating at an angle θ_n relative to z axis. We now introduce the position variable $\rho = \sqrt{x^2 + z^2}$, and define R_n by the relation $R_n = \sqrt{(nk_x)^2 + (k_z^{dB})^2}$. It is also convenient to introduce the diffraction angle θ_n and the tilt angle ξ, as follows:

$$\sin\theta_n = \left[1 + \lambda^2/\left(n\lambda_z^{dB}\cos\alpha^2\right)\right]^{-1/2}, \quad \sin\xi = [1 + (x/z)^2]^{-1/2}. \tag{11}$$

Next we make use of the relation $nk_x x - k_z^{dB} z = \rho R_n \sin(\theta_n + \xi)$, which enables the wave function to be written in the following form:

$$\Psi(r,\phi,0) = \mathcal{N} e^{-iA\tau} e^{-iB\tau} D \times \sum_{n=-\infty}^{\infty} i^n J_n(C\tau) e^{-i\rho R_n \sin(\theta_n+\xi)} e^{inl\phi}. \quad (12)$$

This wave function corresponds to a sum of atomic beams, labeled by the index n carrying orbital angular momenta $\pm nl\hbar$. Note that $l\hbar$ is the orbital angular momentum of the LG beam, which was required to construct the fork diffraction pattern. This angular momentum is seen here as having been transferred to the atomic beams. The situation is depicted schematically in Fig. 1.

The probability distribution associated with a sharp atomic vortex state n is given by

$$p_n(r) = |\langle e^{inl\phi}, \Psi(r,\phi,0)\rangle|^2 \approx e^{-\frac{8\ln 2}{\sigma^2} r^2} |J_n(C\tau)|^2. \quad (13)$$

This distribution function can be explored for different diffraction orders. In the case of lower diffraction orders, we note that the central component $n = 0$, is an Airy-type state function and carries no angular momentum. The radial probability distribution for the first diffraction order $n = 1$ can be shown to be a doughnut-type mode with a characteristic ring shape.

For practical purposes it is desirable to be able to ensure that the atomic vortex beams corresponding to different diffraction orders are well separated in real space with minimum overlap, a requirement that clearly depends on the parameters used to generate the diffraction pattern. From the above discussion it is also seen that the amplitude of a given component depends on the initial-state function and the corresponding Bessel function. For illustration we consider the concrete example of a system of neutral atoms diffracted from a suitably constructed optical mask at far-off resonance with an atomic transition. The transition in question concerns sodium atoms and is identified as $3^2S_{1/2} - 3^2P_{1/2}$, with parameters

$$\tau = 0.8\Gamma^{-1}; \quad \Omega_P = \Gamma; \quad \Omega_{\rm LG} = 1.2\Gamma; \quad w_0 = 1\ \mu{\rm m};$$
$$\lambda_{\rm light} = 589\ {\rm nm}; \quad k_x = 2.1 \times 10^6\ {\rm m}^{-1}; \quad \Delta = 10\Gamma, \quad (14)$$

and the value of k_x shown corresponds to tilting angle $\alpha = \frac{\pi}{16}$ with respect to z axis.

The diffraction process described by the above choice of parameters is a Raman-Nath (RN) diffraction [22]. The criteria for the validity of the RN regime are (i) the width of the initial atomic beam must be large compared with the spatial extent of the diffracting potential (thin grating [23]) and (ii) the transverse kinetic energy of the atoms as they enter the diffraction region should be smaller than the maximum energy of the atom-light interaction. Next we consider the validity of these criteria for the parameter values displayed above in a experimental configuration.

The radial spread of the light field is typically 8 μm and we consider three cases in which the wave packet sizes are the same as those in the experiments performed by Anderson *et al.* [13], namely $\sigma = 21,30,42\ \mu$m, so the first RN criterion is satisfied. Consider next the second RN criterion. For each of these values of σ the Heisenberg uncertainty principle indicates that the corresponding transverse momentum spreads of the wave packets are given. respectively, by

$$\Delta p_\perp \approx \frac{\hbar}{\sigma} = 5.2 \times 10^{-30}, \quad 3.47 \times 10^{-30}, \quad 2.47 \times 10^{-30}\ {\rm kgms}^{-1}. \quad (15)$$

We find, respectively,

$$\Delta E_\perp = \frac{(\Delta p_\perp)^2}{2M} \approx 3.41\hbar,\ 1.52\hbar,\ 0.77\hbar, \quad (16)$$

where the units attached to the numerical factors are s^{-1}. The maximum energy of the atom-light interaction during the diffraction process is estimated to have the following value for all cases:

$$U_{\rm diff} = \frac{2\hbar\Omega_p\Omega_{\rm LG}}{\Delta} = 14.7 \times 10^6\hbar, \quad (17)$$

which confirms that $\Delta E \ll U_{\rm diff}$. So, the second RN criterion is satisfied.

Further interesting aspects of the vortex formation can be explored by looking at the *linear regime* of the diffraction in which relation $\lambda_z^{dB} \ll \lambda$ is valid between the de Broglie wavelength of the incident atom beam and that of the light beam along x axis. Within this approximation, $R_n \approx k_z^{dB}$ and $\theta_n \approx n\theta = n\frac{\lambda_z^{dB}}{\lambda}\cos\alpha$ are valid, i.e., the diffraction angles vary linearly with the angle step θ. In this case we can write

$$\sin(\theta_n + \xi) \approx \sin\xi + n\frac{\lambda_z^{dB}}{\lambda}\cos\alpha\cos\xi, \quad (18)$$

which is valid in the linear regime of atomic diffraction. This relation corresponds to the standard *Bragg diffraction condition* that governs light or particle diffraction in periodic structures, for example in a crystalline solid-state context, in the case of light gratings and microfabricated material gratings. It is responsible for the Kapitza-Dirac effect, which has received experimental implementation (see, e.g., Ref. [23]). The resulting atomic state in the linear regime now reads

$$\Psi(r,\phi,0;\alpha) \approx \mathcal{N} e^{-iA\tau} e^{-iB\tau} D e^{-i\rho k_z^{dB}\sin\xi} \times \sum_{n=-\infty}^{\infty} i^n J_n(C\tau) e^{-in\rho k\cos\alpha\cos\xi} e^{inl\phi}. \quad (19)$$

This describes a set of diffracted atom beams separated by equal angles, with linear orbital angular momentum phase dependence in their amplitudes. The defining relation $\lambda_z^{dB} \ll \lambda$, implies that thermal atoms diffract approximately in the linear regime, while the previously analyzed cool atom beams released from a BEC, not being in the linear regime, are expected to diffract in unequal deflection angles.

Next we consider the process of the detection of the diffracted beams. A necessary condition for detection is derived as follows. Let the beams traveling a distance z after passing through the light mask be deflected by the angle θ_n. The different beams would intersect a circle in the z-x plane of radius z (where z is now defined as the axial distance from the center of the grating) at points on its circumference with arc length $\Delta s_n = z\theta_n \approx nz\theta \approx n\Delta s$, where $\Delta s = z\theta \approx z\frac{\lambda_z^{dB}}{\lambda}\cos\alpha$, is the arc length between two neighboring diffracted beams (i.e., $|n| = 1$)). A high resolution

of the neighboring beams requires that $\Delta s > w_0$, which implies the criterion $\frac{z}{w_0} \ll \frac{\lambda}{\lambda_z^{dB}\cos\alpha}$.

For the parameters chosen above we assume that the atoms entering the light mask have typical speeds of the order $v = 0.01m/s$, i.e. with de Broglie atomic wave number $k_z^{dB} = Mv/\hbar = 5.83 \times 10^8\, m^{-1}$. The separation criterion (for $\alpha = \frac{\pi}{16}$ as before), requires that $z > 0.28\,\mu$m, which then allows reasonable separation for vortex detection.

Recalling that the primary purpose of the optical diffraction grating is to spatially disperse light by wavelength, we suggest that the atomic diffraction setup analyzed here would also function as angular dispersive element for incident atoms based on their de Broglie wavelength. Indeed if the thermal distribution of the incoming atoms has a nonuniform energy (i.e., momentum) profile, then via thermal de Broglie wavelength $\lambda^{dB} \sim \frac{h}{\sqrt{MkT}}$, the temperature distribution will determine the atomic wavelengths along the propagation axis. Physically this would imply that the incident beam is not monochromatic with respect to λ^{dB}, so the transmissive diffraction taking place in the optical mask would result in a wavelength selective angular deflection for the atoms, described by an angle function $\theta_n(\lambda^{dB})$. Differentiation of the grating equation (18), yields the atomic angular dispersion coefficient D_n,

$$D_n = \frac{d\theta_n}{d\lambda_z^{dB}} \approx \frac{n}{\lambda}\frac{\cos\alpha}{\cos(\theta_n + \pi/4)}. \tag{20}$$

Stretching the analogy of atomic diffraction with the diffraction of light by a grating further, we note that the grating equation for light imposes restrictions on the light wavelengths from being diffracted into more than a finite number of orders [24]. By contrast the analogous relation, Eq. (18), for the atomic diffraction imposes restrictions on the number of orders, i.e., the number of atom vortex beams, that do not involve the atomic and light wavelengths. Instead this number is restricted by one of the tilt angles, the ξ only, by the constraint

$$|n| \leqslant \left(1 + \frac{1}{|\sin\xi|}\right). \tag{21}$$

For example, in the special case for which $x = z$ as given by Eq. (11), which corresponds to the tilt angle $\xi = \frac{\pi}{4}$, the possible vortex states are labeled by $n = \{0, \pm1, \pm2\}$. The same vortex states are possible for tilt angles $\xi = \frac{\pi}{3}, \frac{\pi}{4}$, as well. Similarly to the angles $\xi = \frac{\pi}{6}, \frac{\pi}{8}$ corresponds the set $n = \{0, \pm1, \pm2, \pm3\}$, and to $\xi = \frac{\pi}{12}$ corresponds the set $n = \{0, \pm1, \pm2, \pm3, \pm4\}$, etc.

In conclusion we suggest that the realization of atom vortex beams put forward in this work would open up a new area of atom optics in which atoms carrying orbital angular momentum interact with each other, or with other forms of matter. Further studies and various applications should be anticipated. As to theoretical extensions, there is a need to relax some of the restrictions we have introduced, e.g., the Raman-Nath approximation [in order to study the thick grating limit (Bragg diffraction)]; as well as the need to study vortices on the whole transverse plane, i.e., beyond the maximal intensity circle. As to applications, we would include atom interferometry, the functioning of mask as a dispersive prism for de Broglie waves, the encoding and processing of quantum information in atom vorticity, the imaging of neutral samples via atom vortex beams, the interference of atom vortex beams of opposite helicity, and the building of quantum entanglement in the infinite dimensional Hilbert space of atom vortex beam states.

The authors are grateful to Dr. J. Courtial for many useful discussions. They also wish to thank the UK EPSRC Cold Atom Network for funding that enabled a visit by the third named author to the Department of Sciences, Technical University of Crete, Greece where this work was initiated. This project was supported by NSTIP Strategic Technologies Programs, No. 11-MAT-1898-02 in the Kingdom of Saudi Arabia.

[1] L. Allen, M. W. Beijersbergen, R. J. C. Spreeuw, and J. P. Woerdman, Phys. Rev. A **45**, 8185 (1992).
[2] L. Allen, M. J. Padgett, and M. Babiker, Prog. Optics **39**, 291 (1999).
[3] L. Allen, S. M. Barnett, and M. J. Padgett, *Optical Angular Momentum* (IOP Publishing, Bristol, 2003).
[4] D. L. Andrews, *Structured Light and Its Applications. An Introduction to Phase-structured Beams and Nanoscale Optical Forces* (Academic, Burlington, Massachusetts, 2008).
[5] D. L. Andrews and M. Babiker, *The Orbital Angular Momentum of Light* (Cambridge University Press, Cambridge, 2012).
[6] D. G. Grier, Nature (London) **424**, 810 (2003).
[7] M. Babiker, W. L. Power, and L. Allen, Phys. Rev. Lett. **73**, 1239 (1994).
[8] M. Babiker, C. R. Bennett, D. L. Andrews, and L. D. Romero, Phys. Rev. Lett. **89**, 143601 (2002).
[9] A. R. Carter, M. Babiker, M. Al-Amri, and D. L. Andrews, Phys. Rev. A **72**, 043407 (2005); **73**, 021401 (2006).
[10] V. E. Lembessis, D. Ellinas, and M. Babiker, Phys. Rev. A **84**, 043422 (2011).
[11] V. E. Lembessis and M. Babiker, Phys. Rev. Lett. **110**, 083002 (2013).
[12] S. Francke-Arnold, J. Leach, M. J. Padgett, V. E. Lembessis, D. Ellinas, A. J. Wright, J. M. Girkin, and A. S. Arnold, Opt. Express **15**, 8619 (2007).
[13] M. F. Anderson, C. Ryu, P. Clade', V. Natarajan, A. Vasiri, K. Helmerson, and W. D. Phillips, Phys. Rev. Lett. **97**, 170406 (2006).
[14] M. Uchida and A. Tonomura, Nature (London) **464**, 737 (2010).
[15] J. Verbeeck, H. Tian, and P. Schattschneider, Nature (London) **467**, 301 (2010).
[16] B. J. McMorran, A. Agrawal, I. M. Anderson, A. A. Herzing, H. J. Lezek, J. J. McClelland, and J. Unguris, Science **331**, 192 (2011).
[17] K. Y. Bliokh, Y. P. Bliokh, S. Savelev, and F. Nori, Phys. Rev. Lett. **99**, 190404 (2007).

[18] J. Verbeeck, H. Tian, and A. Beche, Ultramicroscopy **113**, 83 (2011).
[19] S. M. Lloyd, M. Babiker, and J. Yuan, Phys. Rev. Lett. **108**, 074802 (2012).
[20] S. M. Lloyd, M. Babiker, and J. Yuan, Phys. Rev. Lett. **110**, 189502 (2013).
[21] W. Ketterle (private communication).
[22] P. Meystre, *Atom Optics* (Springer-Verlag, New York, 2001), pp. 58, 61.
[23] A. D. Cronin, J. Schmiedmayer, and D. E. Pritchard, Rev. Mod. Phys. **81**, 1051 (2009).
[24] C. H. Palmer, *Diffraction Grating Handbook*, 6th ed. (Newport Corporation, Rochester, New York, 2005).